Exceptional Points of Degeneracy and Branch Points for Coupled Transmission Lines—Linear-Algebra and Bifurcation Theory Perspectives

George W. Hanson, *Fellow, IEEE*, Alexander B. Yakovlev, *Senior Member, IEEE*, Mohamed A. K. Othman, *Member, IEEE*, and Filippo Capolino, *Senior Member, IEEE*

***Abstract*— We provide a new angle to investigate exceptional points of degeneracy (EPD) relating the current linear-algebra point of view to bifurcation theory. We apply these concepts to EPDs related to propagation in waveguides supporting two modes (in each direction), described as a coupled transmission line. We show that EPDs are singular points of the dispersion function associated with the fold bifurcation connecting multiple branches of dispersion spectra. This provides an important connection between various modal interaction phenomena known in guided-wave structures with recent interesting effects observed in quantum mechanics, photonics, and metamaterials systems described in terms of the algebraic EPD formalism. Since bifurcation theory involves only eigenvalues, we also establish the connection to the linear-algebra point of view by casting the system eigenvectors in terms of eigenvalues, analytically showing that the coalescence of two eigenvalues results automatically in the coalescence of the two respective eigenvectors. Therefore, for the studied two-coupled transmission-line problem, the eigenvalue degeneracy explicitly implies an EPD. Furthermore, we discuss in some detail the fact that EPDs define branch points in the complex frequency plane, we provide simple formulas for these points, and we show that parity-time (PT) symmetry leads to real-valued EPDs occurring on the real-frequency axis.**

***Index Terms*— Bifurcation theory, branch points (BPs), electromagnetic propagation, electromagnetic theory, exceptional points of degeneracy (EPD), multiconductor transmission lines, transmission lines.**

I. Introduction

When propagation in a coupled-waveguide system is described in terms of a system matrix, exceptional points of degeneracy (EPD) are points in the parameter space of such a system at which simultaneous eigenvalue and eigenvector degeneracies occur [1]. Interest in EPDs has recently risen due to parity-time (PT) symmetric systems, wherein non-Hermitian Hamiltonians can nevertheless exhibit real spectra, representing physical observables. PT symmetry has led to a range of interesting phenomena in quantum mechanics and photonic systems [2]–[10], and in metamaterials research [11]–[14], with applications to cloaking, negative refraction, imaging, field transformation, and sensing, among others. In a system whose evolution is described with a system matrix, EPDs are associated with a Jordan block, corresponding to a deficient (incomplete) set of eigenfunctions, and algebraically growing solutions of generalized (associated) eigenvectors at the EPD. Moreover, in the vicinity of EPDs, by virtue of small detuning, eigenvalues exhibit unconventional perturbations following a fractional power-law expansion in the perturbation parameters [15].

It is important to point out that EPDs are manifest in the parameter space of a system's eigenstates' temporal evolution (e.g., such as certain coupled resonators with loss and gain), or of a system's eigenstates' spatial evolution. This latter case represents the evolution of eigenwaves in a given spatial direction, such as in a multimode waveguide with prescribed loss and gain, which is investigated in this paper, where the multimode waveguide is a pair of uniform coupled transmission lines (CTLs). Some of the earliest examples of EPDs have also been observed in structures with a spatial periodicity which are explored, for instance, in [16]–[19], such as those exhibiting degenerate band edges or stationary inflection points. Although EPDs are usually viewed from a linear-algebra standpoint and are associated with systems described by matrices with Jordan blocks [1], [16], it has been observed that they also represent points in the configuration space where multiple branches of spectra connect and are linked to branch points (BPs) in the space of control variables [20], [21].

In the current literature, EPDs have been investigated in terms of linear-algebra and coupled-mode theory, and the idea of degenerate eigenvectors of a system matrix that is similar to another one that contains a Jordan block as shown in [22]. In this paper, we connect the current linear-algebra approach to

Manuscript received April 22, 2018; revised September 8, 2018; accepted October 21, 2018. Date of publication November 6, 2018; date of current version February 5, 2019. The work of M. A. K. Othman and F. Capolino was supported by the Air Force Office of Scientific Research under Award FA9550-15-1-0280. *(Corresponding author: George W. Hanson.)*

G. W. Hanson is with the Department of Electrical Engineering and Computer Science, University of Wisconsin–Milwaukee, Milwaukee, WI 53211 USA (e-mail: george@uwm.edu).

A. B. Yakovlev is with the Department of Electrical Engineering, The University of Mississippi, University, MS 38677 USA (e-mail: yakovlev@olemiss.edu).

M. A. K. Othman and F. Capolino are with the Department of Electrical Engineering and Computer Science, University of California at Irvine, Irvine, CA 92697-2625 USA (e-mail: mothman@uci.edu; f.capolino@uci.edu).

Color versions of one or more of the figures in this paper are available online at http://ieeexplore.ieee.org.

Digital Object Identifier 10.1109/TAP.2018.2879761

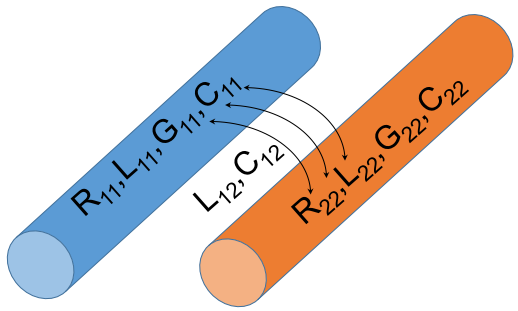

Fig. 1. Two coupled waveguides whose modes are equivalently described in terms of CTLs with mutual capacitive and inductive coupling, invariant along z. They exhibit EPDs under certain conditions described in this paper.

singular points from bifurcation theory, explained in [23]–[26] for multilayer waveguiding systems. We point out that this new point of view emphasizes the connection with BPs of the dispersion spectrum and EPDs and leads to some simple formulas for the location of such EPDs. The provided concepts are general, and in this paper, for simplicity, we consider a coupled uniform transmission-line system with gain and loss, recently examined in [22]. We also demonstrate several new aspects of EPDs in these systems. Specifically, we derive closed-form expressions for the system eigenvalues and eigenvectors, and in particular, we show that the eigenvectors are represented in terms of eigenvalues analytically indicating when the eigenvector degeneracies occur, stressing that for two coupled uniform transmission lines, eigenvalue degeneracies *always* result in eigenvector degeneracies, explicitly implying that *all* eigenvalue degeneracies represent EPDs. Furthermore, we also derive closed-form expressions for the branch-point singularities in the dispersion diagram using bifurcation theory and show the connection with the Puiseux series applied to the degenerate eigenvalues of an EPD. The new point of view of EPDs explained in this paper is connected to previous work on fold-point and branch-point singularities in waveguiding systems [23]–[31], aiming at improving the understanding of EPDs.

Also, we should point out that the analysis in this paper leads to the conclusion that various wave phenomena, like those studied in [23]–[31] for instance, including cutoff regimes in closed-boundary and open-boundary waveguides for bound and leaky waves, and modal interaction and modal transformation in guided-wave structures, are indeed EPD phenomena. This has not been recognized before, and this brings a stronger connection of wave phenomena occurring in microwave devices with interesting effects recently observed in quantum mechanics, photonics, and metamaterials systems.

II. Coupled Transmission-Line Formulation

We consider two uniform CTLs as depicted in Fig. 1. We refer to the formulation given in [22] for the analysis of eigenwaves propagating along the z-direction in a CTL (the $e^{i\omega t}$ time-harmonic evolution is implicitly assumed). Here, we summarize the mathematical steps carried out to obtain the eigenwaves supported by such a guiding system. The CTL equations for a two-line network consisting of uniform transmission lines are given by the telegraphers equations [32], [33]

$$\frac{d\mathbf{V}(z)}{dz} = -\underline{\underline{\mathbf{Z}}}\,\mathbf{I}(z), \quad \frac{d\mathbf{I}(z)}{dz} = -\underline{\underline{\mathbf{Y}}}\,\mathbf{V}(z) \tag{1}$$

where the voltage and current are 2-D vectors, $\mathbf{V}(z) = [V_1(z) \quad V_2(z)]^{\mathrm{T}}$ and $\mathbf{I}(z) = [I_1(z) \quad I_2(z)]^{\mathrm{T}}$, whereas $\underline{\underline{\mathbf{Z}}}$ and $\underline{\underline{\mathbf{Y}}}$ are 2×2 matrices

$$\underline{\underline{\mathbf{Z}}}(\omega) = \begin{bmatrix} Z_{11} & Z_{12} \\ Z_{21} & Z_{22} \end{bmatrix}, \quad \underline{\underline{\mathbf{Y}}}(\omega) = \begin{bmatrix} Y_{11} & Y_{12} \\ Y_{21} & Y_{22} \end{bmatrix} \tag{2}$$

where the off-diagonal elements represent coupling between the two transmission lines. Furthermore, in this paper, we assume that the per-unit-length series impedance and shunt admittance matrices are given by $\underline{\underline{\mathbf{Z}}} = i\omega\underline{\underline{\mathbf{L}}} + \underline{\underline{\mathbf{R}}}$ and $\underline{\underline{\mathbf{Y}}} = i\omega\underline{\underline{\mathbf{C}}} + \underline{\underline{\mathbf{G}}}$, where $\underline{\underline{\mathbf{R}}}, \underline{\underline{\mathbf{G}}}, \underline{\underline{\mathbf{L}}}$, and $\underline{\underline{\mathbf{C}}}$ are the matrices of the per-unit-length distributed CTL parameters, assumed nondispersive for simplicity. The matrices $\underline{\underline{\mathbf{L}}}$ and $\underline{\underline{\mathbf{C}}}$ are the positive definite and symmetric [32], [33], and the off-diagonal entries of $\underline{\underline{\mathbf{C}}}$ and $\underline{\underline{\mathbf{G}}}$ are negative. In general, $\underline{\underline{\mathbf{R}}}$ and $\underline{\underline{\mathbf{G}}}$ are the positive definite if they represent losses (no gain), and in the following, they are assumed to be diagonal for simplicity. In addition, note also that the per-unit-length impedance and admittance matrices may possess cutoff capacitance and inductance terms, respectively, as done in [34, Ch. 7], and also in [35] to model waveguide cutoff. Since we do not investigate cutoff related degeneracies, we simply ignore these terms in the CTL formulations mentioned above.

A. EPD From a Linear-Algebra Perspective

Before presenting the bifurcation theory view of EPD, we summarize the standard linear-algebra perspective of EPD, obtain one new result, and present several aspects that we later connect with bifurcation theory.

Decoupling (1), we obtain two second-order wave equations for the voltage and current vectors

$$\frac{d^2\mathbf{V}(z)}{dz^2} = \underline{\underline{\mathbf{Z}}}\,\underline{\underline{\mathbf{Y}}}\,\mathbf{V}(z), \quad \frac{d^2\mathbf{I}(z)}{dz^2} = \underline{\underline{\mathbf{Y}}}\,\underline{\underline{\mathbf{Z}}}\,\mathbf{I}(z). \tag{3}$$

The two systems lead to the same wavenumber solutions though, in general, $\underline{\underline{\mathbf{Z}}}$ and $\underline{\underline{\mathbf{Y}}}$ do not necessarily commute; one common exception is for lossless lines in a homogeneous environment characterized by μ, ε, in which case $\underline{\underline{\mathbf{Z}}}\,\underline{\underline{\mathbf{Y}}} = -\omega^2\mu\varepsilon\underline{\underline{\mathbf{1}}}$, where $\underline{\underline{\mathbf{1}}}$ is the 2×2 identity matrix. Alternatively, one may form a 4-D state vector $\mathbf{\Psi}(z) = [V_1(z) \quad V_2(z) \quad I_1(z) \quad I_2(z)]^{\mathrm{T}}$, leading to

$$\frac{d}{dz}\mathbf{\Psi}(z) = -i\underline{\underline{\mathbf{M}}}(\omega)\,\mathbf{\Psi}(z) \tag{4}$$

where

$$\underline{\underline{\mathbf{M}}}(\omega) = \begin{bmatrix} \underline{\underline{\mathbf{0}}} & -i\underline{\underline{\mathbf{Z}}} \\ -i\underline{\underline{\mathbf{Y}}} & \underline{\underline{\mathbf{0}}} \end{bmatrix}. \tag{5}$$

Assuming that the transmission line is invariant along z, the homogeneous solutions to (3) and (4) are found to be in the

form $\mathbf{\Psi}(z) \propto e^{-ikz}$ with k being the wavenumber. As such, (3) and (4) become

$$\begin{aligned} -\left(\underline{\underline{\mathbf{Z}}}\,\underline{\underline{\mathbf{Y}}}\right)(\omega)\ \mathbf{V}(z) &= k^2\mathbf{V}(z) \\ -\left(\underline{\underline{\mathbf{Y}}}\,\underline{\underline{\mathbf{Z}}}\right)(\omega)\ \mathbf{I}(z) &= k^2\mathbf{I}(z) \\ \underline{\mathbf{M}}(\omega)\,\mathbf{\Psi}(z) &= k\mathbf{\Psi}(z). \end{aligned} \tag{6}$$

Note that the first two equations in (6) have two eigenvalues k^2 (and both signs of k are possible), whereas the third equation in (6) has four eigenvalues k. All three eigenvalue problems lead to the same four eigenvalues, and encompass the same physics, which is thoroughly explained in [22]. Here, we wish to make several new observations about these eigenproblems from two different but complementary perspectives, which opens up new ways for utilizing such EPDs and conceiving new operational principles for a variety of microwave devices. For simplicity, we assume reciprocity, i.e., $Y_{21} = Y_{12}$ and $Z_{21} = Z_{12}$.

We denote the algebraic multiplicity for eigenvalues λ (i.e., the order of the eigenvalue degeneracy) as $m(\lambda)$. The geometric multiplicity of the eigenvalue (the span of the eigenvector space associated with the eigenvalue) is denoted as $l(\lambda)$.

In order to connect EPDs with singular points of the dispersion diagram and bifurcation theory (both based on eigenvalue behavior), we show that for the systems of two CTLs considered earlier, when an EPD occurs the eigenvalues degeneracy explicitly implies eigenvectors degeneracy. In other words, at an EPD, one has $m(\lambda) > l(\lambda)$, i.e., all degenerate eigenvalues have a deficient eigenspace, and the matrices $\underline{\mathbf{M}}, \underline{\underline{\mathbf{Z}}}\,\underline{\underline{\mathbf{Y}}}, \underline{\underline{\mathbf{Y}}}\,\underline{\underline{\mathbf{Z}}}$ *cannot* be diagonalized (except for the trivial degeneracy at $k = 0$ and in uncoupled lines). In particular, for the two uniform CTLs considered here, EPDs are associated with $l(\lambda) = 1$ and $m(\lambda) = 2$.

To see this, we first consider the 2×2 eigenvalue problem in (6); $-\underline{\underline{\mathbf{Z}}}\,\underline{\underline{\mathbf{Y}}}$ having eigenvalues $k_{1,2}^2$ and *regular* voltage eigenvectors $\mathbf{V}_{1,2}$, obtained analytically as

$$k_n^2 = \frac{1}{2}\left(-T + \nu_n D\right), \quad \mathbf{V}_n = \begin{bmatrix} -\frac{N_2 + k_n^2}{N_1} \\ 1 \end{bmatrix} \tag{7}$$

where $n = 1, 2$, $\nu_n = (-1)^n$, then $N_1 = Y_{11}Z_{12} + Y_{12}Z_{22}$, $N_2 = Y_{22}Z_{22} + Y_{12}Z_{12}$ and

$$D = \sqrt{T^2 - 4\det\left(\underline{\underline{\mathbf{Z}}}\,\underline{\underline{\mathbf{Y}}}\right)}. \tag{8}$$

The trace T and determinant of $\underline{\underline{\mathbf{Z}}}\,\underline{\underline{\mathbf{Y}}}$ are given by

$$T = \mathrm{Tr}\left(\underline{\underline{\mathbf{Z}}}\,\underline{\underline{\mathbf{Y}}}\right) = 2Y_{12}Z_{12} + Y_{22}Z_{22} + Y_{11}Z_{11} \tag{9}$$

$$\det\left(\underline{\underline{\mathbf{Z}}}\,\underline{\underline{\mathbf{Y}}}\right) = \left(Y_{11}Y_{22} - Y_{12}^2\right)\left(Z_{11}Z_{22} - Z_{12}^2\right). \tag{10}$$

For the $-\underline{\underline{\mathbf{Y}}}\,\underline{\underline{\mathbf{Z}}}$ formulation in (6), everything is analogous; the same eigenvalues are obtained, and the regular current $\mathbf{I}_{1,2}$ eigenvectors are retrieved using (7) by replacing $N_1 \rightarrow Y_{22}Z_{12} + Y_{12}Z_{11}$.

It is obvious that, without considering the trivial eigenvalue degeneracy at $k = 0$, eigenvalue degeneracies occur when $D = 0$, and moreover, from (7), it is clear that at this point eigenvectors are also degenerate; $m\left(k^2\right) = 2$ and $l\left(k^2\right) = 1$ since $\mathbf{V}_1 = \mathbf{V}_2$.

For the formulation in (6) involving the 4×4 matrix $\underline{\mathbf{M}}$, one finds the four eigenvalues as

$$k_n = (\pm)\,\tfrac{1}{\sqrt{2}}\sqrt{-T + \nu_n D}, \tag{11}$$

and the four regular eigenvectors as cast in terms of their respective eigenvalues as

$$\mathbf{\Psi}_n = \begin{bmatrix} \frac{-ik_n 2\left(N_2 + k_n^2\right)}{N_3 - \nu_n Y_{12} D} \\ \frac{2ik_n N_1}{N_3 - \nu_n Y_{12} D} \\ \frac{-2\left(N_2 + k_n^2\right)Y_{11} + 2Y_{12}N_1}{N_3 - \nu_n Y_{12} D} \\ 1 \end{bmatrix} \tag{12}$$

where the $+$ sign in front is for $n = 1, 2$, the $-$ sign in front is for $n = 3, 4$,$N_3 = Y_{11}\left(Y_{12}Z_{11} + 2Y_{22}Z_{12}\right) + Y_{12}Y_{22}Z_{22}$, and again both eigenvalues and eigenvectors become simultaneously degenerate when $D = 0$, and $m(\pm k) = 2 > l(\pm k) = 1$.

Therefore, excepting the case of uncoupled identical lines[1] and $k = 0$, for all system descriptions in (6), from (12), it is clear that eigenvector degeneracies are simultaneous with eigenvalue degeneracies. Thus, these simultaneous eigenvalue and eigenvector degeneracies are, by definition, an EPD, where $k = \pm k_e$ with $k \equiv \sqrt{-T}/\sqrt{2}$. Indeed, at such points, the matrices in (6) are deficient and cannot be diagonalized because there are not enough eigenvectors to form a complete basis. From the above-mentioned analysis, we also see that $D = D(\omega)$ clearly represents a square-root type BP in the complex-ω plane. As such, these complex-frequency plane singularities are generally unavailable for monochromatic problems but may be accessed in certain pulse shaping scenarios [36]–[38].

Conditions for EPDs were also presented in [22]; here, we briefly comment on those and the connection with the condition $D = 0$. In [22], it was shown that the conditions

$$T = \mathrm{Tr}\left(\underline{\underline{\mathbf{Z}}}\,\underline{\underline{\mathbf{Y}}}\right) = -2k^2 \tag{13}$$

$$\det\left(\underline{\underline{\mathbf{Z}}}\,\underline{\underline{\mathbf{Y}}}\right) = k^4 \tag{14}$$

are necessary for an eigenvalue degeneracy (and so, in fact, are necessary and sufficient for an EPD as described previously, excepting $k = 0$ and uncoupled lines). These two conditions combined yield $\det\left(\underline{\underline{\mathbf{Z}}}\,\underline{\underline{\mathbf{Y}}}\right) = T^2/4$, which is the condition under which (8) gives $D = 0$.

Furthermore, when, e.g., $\underline{\mathbf{M}}$ is similar to a diagonal matrix (away from the EPD), it can be written in the form

$$\underline{\mathbf{M}} = \underline{\mathbf{U}}\,\underline{\Lambda}\,\underline{\mathbf{U}}^{-1} \tag{15}$$

where $\underline{\mathbf{U}}$ is a 4×4 matrix representing the similarity transformation of $\underline{\mathbf{M}}$ that brings it to a diagonal form, and $\underline{\Lambda}$ is a diagonal matrix whose diagonal entries are the eigenvalues k_n in (11). It was shown in [22] that the condition $\det\left(\underline{\mathbf{U}}\right) = 0$

[1]For uncoupled, non-identical lines ($Z_{12} = Y_{12} = 0$ and $Z_{11} = Z_{22} = Z, Y_{11} = Y_{22} = Y$), $k_1 = \pm\sqrt{-Y_{11}Z_{11}}$, $k_2 = \pm\sqrt{-Y_{22}Z_{22}}$ and $m(k) = l(k) = 2$.

provides necessary and sufficient conditions for an eigenvector degeneracy (at which point the regular eigenvectors must be augmented with associated eigenvectors, and rather than a diagonal form, the simplest matrix representation is given by the Jordan canonical form [39]). Forming

$$\det\left(\underline{\mathbf{U}}\right) = -16\frac{Y_{11}}{N_2^3}D^2\left(Y_{12}Z_{22}+Y_{11}Z_{12}\right)\sqrt{T^2-D^2} = 0 \tag{16}$$

it is observed that $\det\left(\underline{\mathbf{U}}\right) = 0$ occurs when $D = 0$ [or when $Y_{12}Z_{22} + Y_{11}Z_{12} = 0$, which seems to not be of practical interest, and note that $D = T$ cannot be true since, using (8), it would hold only if $\det\left(\underline{\underline{\mathbf{Z}}}\,\underline{\underline{\mathbf{Y}}}\right) = 0$, which is not true]. Alternatively, assuming a similarity transformation analogous to that in (15) but that diagonalizes the 2×2 matrix $-\underline{\underline{\mathbf{Z}}}\,\underline{\underline{\mathbf{Y}}}$

$$\det\left(\underline{\underline{\mathbf{U}}}\right) = -\frac{D}{Y_{11}Z_{12}+Y_{12}Z_{22}} \tag{17}$$

which again occurs at $D = 0$. Therefore, the previously stated conditions in [22] are, for uniform CTLs modeled by nondispersive $\underline{\underline{\mathbf{R}}}$, $\underline{\underline{\mathbf{G}}}$, $\underline{\underline{\mathbf{L}}}$, and $\underline{\underline{\mathbf{C}}}$ parameters, alternative ways of stating the $D = 0$ EPD condition.

Jordan Block and Generalized Eigenvectors. At an EPD, in a uniform 2-CTL, the eigenvalue degeneracy corresponds to an eigenvector degeneracy as we have previously discussed. This can also be shown by noticing that when the eigenvalues of a 2×2 system matrix, as in the first two systems in (6), are identical then it is either proportional to an identity matrix (hence, with two independent eigenvectors), or otherwise, it must be proportional to a 2×2 Jordan block (that exhibit the eigenvector degeneracy). For the 4×4 system matrix $\underline{\mathbf{M}}$ as in the third system in (6), the situation is more involved. At an EPD, the system matrix $\underline{\mathbf{M}}$ is similar to a matrix containing two Jordan blocks as

$$\underline{\mathbf{M}} = \underline{\mathbf{U}}\begin{bmatrix}\underline{\underline{\mathbf{J}}}_+ & \underline{\underline{\mathbf{0}}}\\ \underline{\underline{\mathbf{0}}} & \underline{\underline{\mathbf{J}}}_-\end{bmatrix}\underline{\mathbf{U}}^{-1}, \qquad \underline{\underline{\mathbf{J}}}_\pm = \begin{bmatrix}\pm k_e & 1\\ 0 & \pm k_e\end{bmatrix} \tag{18}$$

where $\underline{\mathbf{U}}$ is a 4×4 matrix constituting a similarity transformation and containing the eigenvectors and the generalized eigenvectors of $\underline{\mathbf{M}}$, namely, $\underline{\mathbf{S}} = \left[\boldsymbol{\Psi}_1 \mid \boldsymbol{\Psi}_1^g \mid \boldsymbol{\Psi}_3 \mid \boldsymbol{\Psi}_3^g\right]$ that are constructed through the Jordan chain procedure ([22], [40], see also [41] for the differential operator case)

$$\left(\underline{\mathbf{M}} - k_e\underline{\mathbf{1}}\right)\boldsymbol{\Psi}_1 = 0, \qquad \left(\underline{\mathbf{M}} - k_e\underline{\mathbf{1}}\right)\boldsymbol{\Psi}_1^g = \boldsymbol{\Psi}_1 \tag{19}$$

$$\left(\underline{\mathbf{M}} + k_e\underline{\mathbf{1}}\right)\boldsymbol{\Psi}_3 = 0, \qquad \left(\underline{\mathbf{M}} + k_e\underline{\mathbf{1}}\right)\boldsymbol{\Psi}_3^g = \boldsymbol{\Psi}_3 \tag{20}$$

with $\boldsymbol{\Psi}_1$ and $\boldsymbol{\Psi}_1^g$ being the regular and generalized eigenvectors associated with the wavenumber k_e at the second-order EPD, and similarly, $\boldsymbol{\Psi}_3$ and $\boldsymbol{\Psi}_3^g$ are the regular and generalized eigenvectors associated with the wavenumber $-k_e$.

We consider the general solution of (4) subject to an initial condition at an arbitrary $z = z_0$ given by $\boldsymbol{\Psi}(z_0) = \boldsymbol{\Psi}_0$. Its general and unique solution is given by

$$\begin{aligned}\Psi(z) &= \exp(-i\underline{\mathbf{M}}z)\Psi_0\\ &= \underline{\mathbf{U}}\begin{bmatrix}\exp(-i\underline{\underline{\mathbf{J}}}_+ z) & \underline{\underline{\mathbf{0}}}\\ \underline{\underline{\mathbf{0}}} & \exp(-i\underline{\underline{\mathbf{J}}}_- z)\end{bmatrix}\underline{\mathbf{U}}^{-1}\Psi_0\end{aligned} \tag{21}$$

where

$$\exp(-i\underline{\underline{\mathbf{J}}}_\pm z) = \begin{bmatrix}e^{\mp ik_e z} & \mp ize^{\mp ik_e z}\\ 0 & e^{\mp ik_e z}\end{bmatrix} \tag{22}$$

which provides growing eigenmodes solutions along z as $\boldsymbol{\Psi}(z) \propto ze^{-ik_e z}$ discussed in [22]. These eigenmodes associated with the generalized eigenvectors grow in space while having a purely real wavenumber. In the vicinity of an EPD, all system matrices $\underline{\underline{\mathbf{Z}}}\,\underline{\underline{\mathbf{Y}}}$, $\underline{\underline{\mathbf{Y}}}\,\underline{\underline{\mathbf{Z}}}$, and $\underline{\mathbf{M}}$ can be diagonalized, and formally, there are four eigenmodes with four different wavenumbers with no algebraic growth. The concept of "vicinity" must be understood as working at a frequency very close to the EPD one, or when a geometrical/physical parameter is perturbed, so the system is not exactly at its EPD. For example, when slightly varying frequency away from the EPD frequency, two modes have eigenvectors (i.e., polarization or voltage/current states) that are not identical but are close to coalescing, i.e., they are almost parallel. This has the important consequence that when the waveguide is terminated, the eigenvectors can hardly provide the necessary field continuity at the ports, causing a giant excitation of fields inside the waveguide working at or in the proximity of an EPD. This has led to the concept of "giant" resonances [17], [42].

Puiseux Series. In what follows, we show that the Puiseux series (also called fractional power expansion series) describes the perturbation of the four eigenvalues (the four wavenumbers) in the vicinity of an EPD when the two transmission-line system is perturbed, i.e., a small perturbation occurs in one or both the matrices $\underline{\underline{\mathbf{Z}}}$ and $\underline{\underline{\mathbf{Y}}}$ in (2) or in the matrix $\underline{\mathbf{M}}$ in (5). In general, a perturbation could be a system parameter $\boldsymbol{\xi}$ or a small deviation of the operational angular frequency ω from the EPD one ω_e. The Puiseux series is a direct consequence of the Jordan Block form (see [15, p. 65]), hence, it is always relevant in systems that exhibit an EPD to describe the eigenvalue perturbation away from the EPD.

It is useful to cast the eigenvalue problems (6) in the form

$$H(k,\omega) = \det\left(\mathbf{A}(\omega,\boldsymbol{\xi}) - k\mathbf{1}\right) = 0 \tag{23}$$

where $\boldsymbol{\xi}$ is the vector of geometrical and material parameters of the system, and $\mathbf{1}$ is the identity matrix. In particular, in the following, all the partial derivatives in ω could be substituted with partial derivatives in $\boldsymbol{\xi}$ and analogous conclusions would be reached relative to the dispersion diagram $(k, \boldsymbol{\xi})$. In (23), the matrix $\mathbf{A}$ represents either the 2×2 system for which $\underline{\underline{\mathbf{A}}} = -\underline{\underline{\mathbf{Z}}}\,\underline{\underline{\mathbf{Y}}}$ or $\underline{\underline{\mathbf{A}}} = -\underline{\underline{\mathbf{Y}}}\,\underline{\underline{\mathbf{Z}}}$ (in which case the eigenvalue is k^2 rather than k) or the 4×4 system $\underline{\mathbf{A}} = \underline{\mathbf{M}}$. In the following, we suppress the dependence on $\boldsymbol{\xi}$ since we provide concepts pertaining to the (k, ω) dispersion diagram. The condition (23) leads to

$$k^4 + k^2\mathrm{Tr}\left(\underline{\underline{\mathbf{A}}}\right) + \det\left(\underline{\underline{\mathbf{A}}}\right) = 0 \tag{24}$$

which is also given in [22]. Denoting derivatives as

$$H_\varsigma^{(m)}(k_e,\omega_e) = \left.\frac{\partial^{(m)}H(k,\omega)}{\partial\varsigma^m}\right|_{(k_e,\omega_e)} \tag{25}$$

for $\varsigma = k, \omega$, an mth-order eigenvalue degeneracy [i.e., an mth-order root of $H(k,\omega)$] will satisfy

$$H(k_e,\omega_e) = H_k'(k_e,\omega_e) = \ldots = H_k^{(m-1)}(k_e,\omega_e) = 0 \quad (26)$$

$$H_k^{(m)}(k_e,\omega_e) \neq 0 \quad (27)$$

where k_e is the degenerate wavenumber and ω_e is the frequency at which the wavenumbers become degenerate. For a second-order EPD, the condition $H_k'(k,\omega) = 0$ is

$$k\left(T + 2k^2\right) = 0 \quad (28)$$

which is equivalent to the trace condition (13) for $k \neq 0$ and leads to $k = \pm\sqrt{-T}/\sqrt{2}$, consistent with the general eigenvalue at the EPD. As described briefly in [22] but of more direct importance here, the eigenvalues of the CTL at such a degeneracy can be written as a convergent Puiseux series [15], [43]

$$k_n(\omega) = k_e + \alpha_1\zeta^n(\omega-\omega_e)^{\frac{1}{m}} + \sum_{p=2}^{\infty}\alpha_p(\zeta^n(\omega-\omega_e)^{\frac{1}{m}})^p \quad (29)$$

for $n = 0, 1, 2, \ldots, m-1$, where $\zeta = e^{i\frac{2\pi}{m}}$. The first-order coefficient is given by

$$\alpha_1 = \left(-\frac{H_\omega'(k_e,\omega_e)}{\frac{1}{m!}H_k^{(m)}(k_e,\omega_e)}\right)^{\frac{1}{m}}. \quad (30)$$

Applying the fractional power expansion (29) to the second-order EPD in the uniform CTL mentioned above, and ignoring expansion terms with order equal or higher than $\omega - \omega_e$, one arrives at

$$k(\omega) \simeq k_e \pm \alpha_1\sqrt{(\omega-\omega_e)} + O(\omega-\omega_e). \quad (31)$$

The first two terms in (31) show the occurrence of the branch-point singularity in the complex-frequency plane, resulting from the square-root function. Associated with this series is the condition [43]

$$H_\omega'(k_e,\omega_e) \neq 0 \quad (32)$$

and so the first-order coefficient α_1 is nonzero. An important aspect of the Puiseux series is that it provides the characteristic form of the solution in the vicinity of the EPD, as shown later. The conditions (26), (27), and (32) will be reconsidered in Section II-B from the viewpoint of singularity and bifurcation theory.

It should be noted that the conditions $H(k_e,\omega_e) = H_k'(k_e,\omega_e) = 0$ are sufficient to define second-order degenerate eigenvalues and simultaneously degenerate eigenvectors, i.e., the EPD. However, the nonzero condition (32) is not otherwise apparent from the linear-algebra formalism. This condition is pronounced only by invoking the Puiseux-series expansion at the EPD, which also clearly demonstrates that the EPD corresponds to a BP in the complex space of frequency (or other parameters). Moreover, the condition (32) will be found to be important to the bifurcation theory view discussed later.

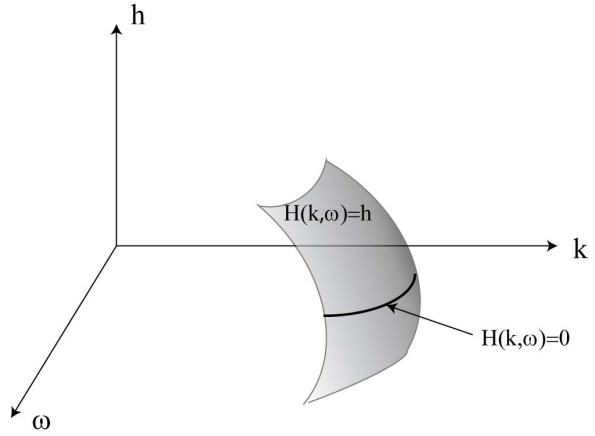

Fig. 2. Depiction of the surface defined by $H(k,\omega) = h$, for $(k,\omega,h) \in \mathbb{R}$. The surface $H(k,\omega) = h$ may intersect the (k,ω)-plane, at $H(k,\omega) = 0$, resulting in the curved line of intersection shown that represents a standard dispersion diagram. If $H(k,\omega) = 0$ does not have solutions for $(k,\omega) \in \mathbb{R}$, then solutions can be found in the complex space.

B. EPD From a Theory of Singular and Bifurcation Points Perspective

In this section, we connect the previous linear-algebra-based analysis with an entirely different method based on singularity and bifurcation theory [44], [45]. We consider the implicit dispersion equation (23), $H(k,\omega) = \det(\mathbf{A}(\omega) - k\mathbf{1}) = 0$. Furthermore, here, $H(k,\omega)$ is more generally understood as a mapping $\mathbb{C}^2 \to \mathbb{C}$ by setting $H(k,\omega) = h$. Obviously, the modal solutions of interest occur for $h = 0$, although viewing H more generally as a mapping facilitates the analysis below. For many waveguiding structures, one must solve $H(k,\omega) = 0$ numerically, via a complex-plane root search, but for the CTLs of interest here, an explicit solution can be obtained, $k_n(\omega) = (\pm)\frac{1}{\sqrt{2}}\sqrt{-T+\nu_n D}$, as given in (11). We recall that based on (12), wavenumber degeneracy implies also eigenvector degeneracy.

The mapping $H(k,\omega) = h$ defines a surface in $\mathbb{C}^2$, and for the simple case of $(k,\omega,h) \in \mathbb{R}$, this is depicted in Fig. 2. The particular case of $H(k,\omega) = 0$ defines a curve (solid line in Fig. 2), which is the dispersion curve of interest, and the smoothness of that curve at a given point determines important modal properties. In particular, one can define regular and singular points of the curve associated with certain modal behavior [23]–[26]. In the following, we consider k as the unknown and ω as a distinguished parameter, although the roles can also be reversed.

We first define a regular point on the curve $H(k,\omega) = 0$ as a point where $\partial H/\partial k \neq 0$. At a regular point, the implicit function theorem [46] can be used to show that a unique smooth curve $k = k(\omega)$ exists in the neighborhood of the point. Except for a finite number of nonregular points (a set of measure zero), all points of modal dispersion are regular points, wherein the dispersion curve is smooth and single valued. It is also worthwhile to note that differentiation $d/d\omega$ of $H(k,\omega) = 0$ leads to, via the chain rule

$$\frac{dk}{d\omega} = -\frac{\partial H/\partial\omega}{\partial H/\partial k} \quad (33)$$

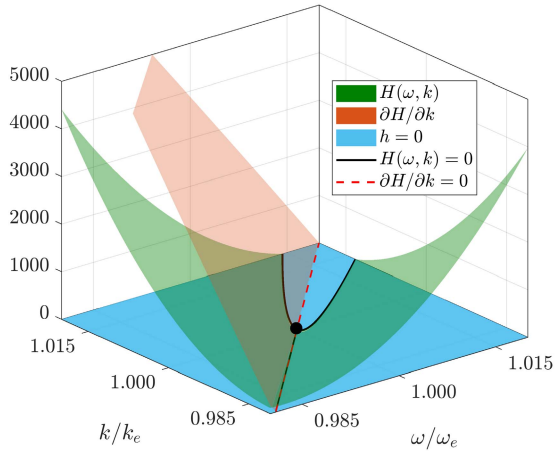

Fig. 3. Functions $H(k,\omega)$ (green), $H'_k(k,\omega)$ (pink), and the zero plane (blue) versus k,ω in the vicinity of the EPD (solid dot). The 2-D dispersion $H(k,\omega)=0$ is also shown (black solid line). The red dashed line is $H'_k(k,\omega)=0$. Units of $H(k,\omega)$ (green) and $H'_k(k,\omega)$ (pink) are in m^{-4} and m^{-3}, respectively.

and therefore, at a regular point, the tangent of $k(\omega)$ (related to the group velocity) is well defined. However, of particular interest are the singular points [26] of the mapping H, which ultimately lead to BPs in the complex-frequency plane [24], [27]. The point (k_s,ω_s) is said to be a singular point of the mapping H if [45, p. 2]

$$H(k_s,\omega_s)=H'_k(k_s,\omega_s)=0. \tag{34}$$

Obviously, in this case, the tangent (33) is undefined. In [45, p. 45], it is shown that $H'_k(k_s,\omega_s)=0$ is a necessary condition for the solution of $H(k_s,\omega_s)=0$ to be a bifurcation point (a point where the number of solutions changes, if considering real solutions—when complex solutions are allowed, the number of solutions is conserved). For the two CTLs described earlier, Fig. 3 shows a plot of $H(k,\omega)$ in the vicinity of the EPD $(k_s,\omega_s)=(k_e,\omega_e)$ (the green, curved surface; numerical values of the CTL parameters are the same as given in Section II-C). The intersection with the zero plane (blue solid) is clearly visible, which forms the dispersion curve; the 2-D dispersion is shown as the black solid line which forms a parabola and a straight-line segment (see also [22, Fig. 4(a)]). A plot of the function $H'_k(k,\omega)$ is also shown in Fig. 3 (the slanted orange plane); units of $H(k,\omega)$ (green) and $H'_k(k,\omega)$ (pink) are in m^{-4} and m^{-3}, respectively. The intersection of $H'_k(k,\omega)$ with the $h=0$ plane forms the line $H'_k(k,\omega)=0$ shown in the figure with a red dashed curve that runs down the middle of the parabola and continues past the apex of the parabola. The intersection of $H(k,\omega)$ and $H'_k(k,\omega)$ on the blue $h=0$ plane is at the singular point (EPD) denoted by a black solid circle. Note that, for $\omega<\omega_e$, the black solid and red dashed curves seem to overlap; this is merely due to the scale of the plot; the two lines (red dashed and black solid) actually only intersect at the EPD, and are not actually parallel for $\omega<\omega_e$. For both H and H'_k, the real part of the function is shown, as the imaginary parts are negligible.

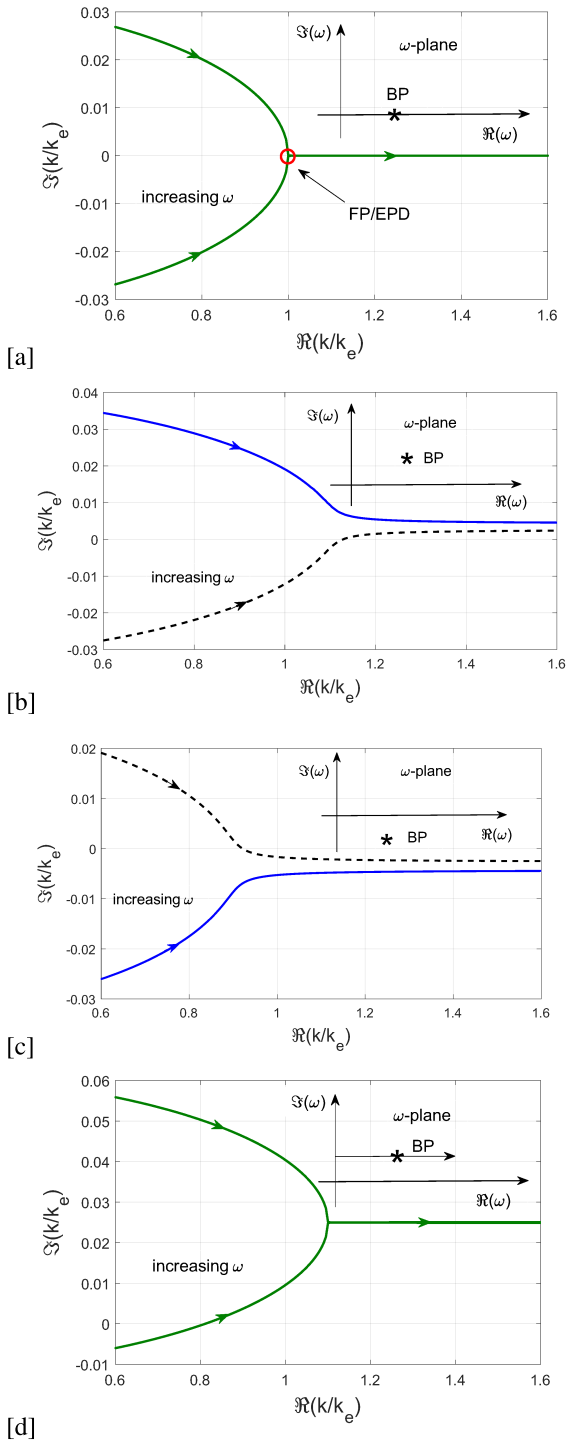

Fig. 4. Dispersion behavior near an EPD for CTLs with (a) $R_{11}=-R_{22}=-73.172$ ohms (PT-symmetric case), as ω varies from $0.5\omega_e$ to $1.5\omega_e$ along the real-ω axis. (b) Same as (a) but for $R_{11}=-1.2R_{22}$, where the EPD lies above the real-frequency axis. (c) Same as (a) but for $R_{11}=-0.8R_{22}$, such that the EPD is below the real-frequency axis. (d) Same as (b) but for $\Re(\omega)$ varying from $0.5\omega_e$ to $1.5\omega_e$ at a constant value $\Im(\omega)=\Im(\omega_s)=(0.022\omega_e)$. In all cases, the pair (k_e,ω_e) is the values at PT symmetry, $(k_e,\omega_e)=(28.649\,\mathrm{m}^{-1},2\pi\,10^9\,\mathrm{s}^{-1})$, $R_{22}=73.172$ ohms, and the star indicates the BP/EPD.

In addition to the conditions (34), we defined a fold bifurcation point (also known as a turning point or limit point) when H satisfies (34) together with [44], [45]

$$H''_{kk}(k_s,\omega_s)H'_{\omega}(k_s,\omega_s)\neq 0 \tag{35}$$

which is the result of the nonzero Jacobian determinant formed from H and H'_k at (k_s, ω_s). The zero conditions (34) together with the nonzero condition $H''_{kk}(k_s, \omega_s) \neq 0$ indicates that the degeneracy is of second order, i.e., where two modal eigenvalues coalesce, as given in (26) and (27). The nonzero condition $H'_\omega(k_s, \omega_s) \neq 0$ serves as a sufficient condition for ω_s to be a BP in the complex ω-plane, as proved in [24] using the Weierstrass preparation theorem. In [23]–[26], [28], and [47], the importance of fold singular points in modal interaction phenomena on guided-wave structures has been addressed in connection with the fold bifurcation from bifurcation theory [44], [45].

Notably, the zero and nonzero conditions (34) and (35) are the same as (26) and (27), and (32) that arise from linear-algebra analysis. Thus, it can be concluded that the fold singular point considered in, e.g., [23]–[26], [28], [47] is in fact an EPD which may reside generally in the complex plane $(k, \omega) \in \mathbb{C}^2$. Therefore, in the following, we denote (k_s, ω_s) as (k_e, ω_e). An analogous treatment of EPDs using the conventional coupled-mode theory [48] is briefly outlined in the Appendix.

Characteristic Form. In the local neighborhood of the fold point (FP)/EPD (k_e, ω_e), the qualitative behavior of the mapping H can be represented by the normal form [44, pp. 308–309] , [45, pp. 196–198]

$$\begin{aligned} &(k-k_e)^2 + (\omega - \omega_e) = 0, \quad \Delta > 0 \\ &(k-k_e)^2 - (\omega - \omega_e) = 0, \quad \Delta < 0 \end{aligned} \tag{36}$$

where $\Delta = H''_{kk}(k_e, \omega_e) H'_\omega(k_e, \omega_e)$, leading to the dispersion function

$$\begin{aligned} &k(\omega) = k_e \pm i\sqrt{\omega - \omega_e}, \quad \Delta > 0 \\ &k(\omega) = k_e \pm \sqrt{\omega - \omega_e}, \quad \Delta < 0. \end{aligned} \tag{37}$$

For the case of $\Delta > 0$ with $\omega < \omega_e$, two branching solutions $\Re(k(\omega))$ of $(k-k_e)^2 + (\omega - \omega_e)$ generate a parabola, and for $\omega > \omega_e$, two equal solutions $\Re(k(\omega))$ exist as a straight line $k(\omega) = k_e$. This corresponds to the characteristic intersection of a parabola and a straight line that occurs at a point of fold bifurcation [44], [45], as shown in Fig. 3 (see also [22]). When $\omega = \omega_e$, there is only one solution (k_e, ω_e) corresponding to the FP. Also, $\Im(k(\omega))$ for $\omega < \omega_e$ yields the solution $k(\omega) = 0$, and for $\omega > \omega_e$, two branching solutions form a parabola in the imaginary plane of $k(\omega)$. A similar analysis can be applied to the case of $\Delta < 0$.

It should be noted that the conditions (34) and (35) define both real and complex FPs/EPDs, however, the normal form (36) is applicable for real-valued FPs, where Δ is real-valued. Otherwise, the quantitative behavior of the local structure of the function $H(k, \omega)$ in the vicinity of FP/EPD can be obtained with a Taylor series expansion. Explicitly, the Taylor series in the vicinity of the EPD can be written as

$$\begin{aligned} H(k,\omega) = {} & H(k_e,\omega_e) + H'_k(k-k_e) + H'_\omega(\omega-\omega_e) \\ & + \frac{1}{2}H''_{kk}(k-k_e)^2 + H''_{k\omega}(k-k_e)(\omega-\omega_e) \\ & + \frac{1}{2}H''_{\omega\omega}(\omega-\omega_e)^2 + \ldots = 0. \end{aligned} \tag{38}$$

Since $H(k_e, \omega_e) = H'_k(k_e, \omega_e) = 0$, and discarding the higher order terms

$$\begin{aligned} k - k_e \simeq {} & \pm\alpha_1(\omega-\omega_e)^{1/2} + \alpha_2(\omega-\omega_e) \\ & \pm\alpha_3(\omega-\omega_e)^{3/2} + O((\omega-\omega_e)^2) \end{aligned} \tag{39}$$

where

$$\alpha_1 = \sqrt{-2\frac{H'_\omega}{H''_{kk}}}, \quad \alpha_2 = -\frac{H''_{\omega k}}{H''_{kk}}, \quad \alpha_3 = \frac{\alpha_1}{2}\frac{(H''_{\omega k})^2 - H''_{\omega\omega}H''_{kk}}{-2H'_\omega H''_{kk}}. \tag{40}$$

The coefficient α_1 is the same as occurs in the Puiseux series (30), and the higher order coefficients are the same as given in [43] retaining the same order of terms.

C. EDPs Leading to Branch Points in the Complex-Frequency Plane

One benefit of the bifurcation view is that it makes clear that, in general, BPs/EPDs are complex-frequency phenomena, identified as singular points of mappings. With this understanding, either solving $D = 0$, or using the conditions that define a fold bifurcation point (34), (35), leads to the frequency where the BP/EPD occurs [this also can be obtained by substituting $k^2 = -T/2$ from (13) into (14)]. Assuming for simplicity that $\underline{\underline{\mathbf{G}}} = \underline{\underline{\mathbf{0}}}$, this leads to

$$\omega_e^2 a + \omega_e b + c = 0 \tag{41}$$

where for $L_{11} = L_{22} = L$ and $C_{11} = C_{22} = C$ (C_{nm} is the nmth element of the capacitance matrix)

$$\begin{aligned} a &= 4(C_{12}L + CL_{12})^2 \\ b &= -4iC_{12}(CL_{12} + LC_{12})(R_{11} + R_{22}) \\ c &= -2R_{22}R_{11}\left(2C_{12}^2 - C^2\right) - C^2\left(R_{11}^2 + R_{22}^2\right). \end{aligned} \tag{42}$$

If $(R_{11} + R_{22}) \neq 0$, then ω_e will not be on the real-ω axis, assuming $(CL_{12} + LC_{12}) \neq 0$.

For the PT-symmetric case, $R_{11} = -R = -R_{22}$

$$\omega_e = \sqrt{\frac{-c}{a}} = R\frac{\sqrt{C^2 - C_{12}^2}}{C_{12}L + CL_{12}}. \tag{43}$$

This will occur on the real-ω axis, since one expects $C^2 > C_{12}^2$. Note that, from a design point of view, expression (43) leads to the needed value of R for a desired value of ω_e.

If we assume that $\underline{\underline{\mathbf{G}}} \neq \underline{\underline{\mathbf{0}}}$, for $L_{11} = L_{22} = L$, $C_{11} = C_{22} = C$, and the PT-symmetric case, $R_{11} = -R = -R_{22}$ and $G_{11} = -G = -G_{22}$

$$\omega_e^2 = -\frac{G^2L_{12}^2 + R^2C_{12}^2 - X - \left(G^2L^2 + C^2R^2\right)}{(CL_{12} + LC_{12})^2}$$

where $X = 2GR(LC + C_{12}L_{12})$. If $R = 0$

$$\omega_e = \frac{G\sqrt{L^2 - L_{12}^2}}{C_{12}L + CL_{12}} \tag{44}$$

which is the dual of (43).

As an example, Fig. 4 shows $\Im(k/k_e)$ versus $\Re(k/k_e)$ in the vicinity of the FP for numerical parameters taken

from [22] corresponding to two coupled microstrip lines (strip width 3 mm, gap between strips 0.1 mm; substrate height 0.75 mm, and dielectric constant of 2.2); $C_{11} = C_{22} = C = 0.12$ nF/m, $L_{11} = L_{22} = L = 0.18\ \mu$H/m, $L_{12} = L_{21} = 49.24$ nH/m, $C_{12} = C_{21} = -25.83$ pF/m, and $\underline{\underline{\mathbf{G}}} = \underline{\underline{\mathbf{0}}}$. Setting a target frequency of $\omega_e = 2\pi\, 10^9\ \mathrm{s}^{-1}$, from (43), to place the EPD on the real frequency axis at ω_e requires $R_{11} = -R_{22} = -73.172$ ohms. The corresponding value of wavenumber at the EPD is $k_e = 28.649\ \mathrm{m}^{-1}$. A 2-D root search of (34) and (35) yields $(k_s/k_e, \omega_s/\omega_e) = (1, 1)$ as expected. Dispersion behavior in the vicinity of the FP is shown in Fig. 4(a). Note that Fig. 4 is not the same as the figures in [22]. In [22], the role of complex frequency was not accessed, whereas Fig. 4 shows what happens when the frequency scan is above, below, or through the complex-frequency BP/EPD as complex frequency is varied.

For other values of $R_{11} = -R_{22}$ (i.e., maintaining PT symmetry), the FP remains on the $\Re(\omega)$ axis but moves to lower or higher frequencies as indicated in (43). Upon breaking PT symmetry by using $R_{11} \neq -R_{22}$, the BP/EPD does not occur on the real-frequency axis, as shown in Fig. 4(b)–(d), where in all cases $R_{22} = 73.172$ ohms. For $R_{11} = -1.2R_{22}$, the 2-D root search of (34) and (35) yields $(k_s/k_e, \omega_s/\omega_e) = (1.1 + i0.025, 1.1 + i0.022)$, where (k_e, ω_e) are the values given earlier under the PT-symmetry conditions, $(k_e, \omega_e) = (28.649\ \mathrm{m}^{-1}, 2\pi\, 10^9\ \mathrm{s}^{-1})$. As such, the EPD lies above the real-frequency axis, and Fig. 4(b) shows the corresponding dispersion behavior. Since a scanning of an operating frequency (assumed real) does not pass through the BP, the eigenvalues do not become degenerate. Alternatively, Fig. 4(c) shows the dispersion behavior when $R_{11} = -0.8R_{22}$, such that the EPD is below the real-frequency axis and the modes have interchanged with their counterparts in Fig. 4(b). Fig. 4(d) shows the dispersion behavior for the case $R_{11} = -1.2R_{22}$, when the real part of frequency is varied while keeping a constant $\Im(\omega) = \Im(\omega_s) = (0.022\omega_e)$, and so passing through the singular point (EPD), at which point the modal degeneracy is recovered at a complex-valued k. In this complex, frequency case a BP is clearly visible and occurs at a complex value wavenumber. Regarding Fig. 4(b) and (c), note that to interchange the modal solutions, it is not necessarily to encircle the EPD/BP (as done in, for example [7], [8]). It is shown in Figs. 4(b) and (c) that the interchange of solutions is due to varying the frequency path above or below the BP [27], [31].

III. Conclusion

For all multimode waveguiding systems that can be equivalently described in terms of two uniform CTLs as shown in Section II, we have explained the concept of EPDs from a point of view based on singular FPs from bifurcation theory and connected this to the current linear-algebra perspective of EPDs. We have also demonstrated that for this class of CTLs, in the framework of the eigenvalue problem, eigenvalue degeneracies are always coincident with eigenvector degeneracies, such that all eigenvalue degeneracies correspond to EPDs. We have discussed the fact that EPDs are related to branch-point singularities in the complex-frequency plane, as can be ascertained from both linear-algebra concepts and from the theory of singular points of complex mappings and bifurcation theory. We have presented simple closed-form expressions for the complex-frequency plane EPDs and showed that under PT symmetry, these BPs reside on the real-frequency axis and generalized the BP discussion to complex frequency and wavenumbers. Finally, we have demonstrated the relationship of the bifurcation theory view with coupled-mode theory.

EPDs in coupled-mode systems as in this paper, with distributed loss and gain, may find various applications in leaky-wave antenna systems, where distributed loss represents distributed radiated power leakage on one transmission line while gain elements are distributed on the other as briefly shown in [22] and [49]. Also, circumventing the BP in a parameter space (e.g. in Section II-A, that may represent a varying coupling or a physical dimension along the transmission lines) may have applications in active mode conversion as shown in [7] and [8], noting that when one encircles a BP does not return to the same position. All these applications shall be investigated in the future studies. The EPD point of view connected to bifurcation theory may also enable new understanding of mode transition by varying frequency or any other parameter. Note that now that we have established the formal connection between EPD and bifurcation theory in uniform waveguides, development of the findings in this paper could be applied also to lossless periodic waveguiding systems that support EPDs, like those shown in [16], [17], [42], [50], and [51] (that do not require gain and loss), expanding the range of applications of EPDs. Since this paper clearly shows the equivalence of the critical point formulation and the traditional algebraic one to describe and EPD, it also enables the recognition of second-order EPDs by the simple knowledge of the dispersion relation via a transcendental equations without resorting to the knowledge of the state vector, and this may find various applications in finding EPDs in many well-known electromagnetic systems.

Appendix: Coupled-Mode Theory

In addition to the transmission-line treatment of EPDs, here, we briefly comment on the matrix that arises from conventional so-called "coupled-mode theory" [48]. For simplicity, we consider the PT-symmetric case for otherwise identical individual transmission lines (e.g., one will have loss and one will have gain). Then, the individual (uncoupled) lines have propagation constants β and β^*, which, when brought into proximity, become $\beta + \delta$ and $\beta^* + \delta^*$ under the coupling constant κ. The coupled system modes obey the evolution equation [52]

$$i\frac{d}{dz}\begin{bmatrix} a_1 \\ a_2 \end{bmatrix} = \begin{bmatrix} \beta + \delta & \kappa \\ \kappa^* & (\beta + \delta)^* \end{bmatrix}\begin{bmatrix} a_1 \\ a_2 \end{bmatrix} = \underline{\underline{\beta}}\begin{bmatrix} a_1 \\ a_2 \end{bmatrix} \quad (45)$$

where a_1 and a_2 are the wave amplitudes in transmission lines 1 and 2, respectively. One can proceed with examination of the eigenvectors and eigenvalues, but it suffices to consider, analogous to (23), the dispersion

relation

$$H(k,\omega) = \left| \begin{bmatrix} \beta(\omega)+\delta(\omega) & \kappa(\omega) \\ \kappa^*(\omega) & (\beta(\omega)+\delta(\omega))^* \end{bmatrix} - k \begin{bmatrix} 1 & 0 \\ 0 & 1 \end{bmatrix} \right| = 0$$
$$= k^2 - k\mathrm{Tr}\left(\underline{\underline{\beta}}\right) + \det\left(\underline{\underline{\beta}}\right) = 0 \quad (46)$$

where $\underline{\underline{\beta}}$ is the 2×2 matrix in (45). Obviously, (46) is analogous to (24). Furthermore

$$H_k'(k,\omega) = 2k - \left(\beta^* + \delta^* + \beta + \delta\right) = 0 \quad (47)$$

leads to

$$k = \frac{1}{2}\left(\beta^* + \delta^* + \beta + \delta\right) = \Re\left(\beta + \delta\right) = \frac{1}{2}\mathrm{Tr}\left(\underline{\underline{\beta}}\right) \quad (48)$$

and using (46), one obtains

$$\mathrm{Tr}^2\left(\underline{\underline{\beta}}(\omega)\right) - 4\det\left(\underline{\underline{\beta}}(\omega)\right) = 0 \quad (49)$$

which is the condition $D = 0$ in (8), and which leads to the value of the EPD frequency $\omega = \omega_\mathrm{e}$. The nonzero condition $H_\omega'(k,\omega) \neq 0$ can be evaluated if all matrix entries are known as a function of frequency. Thus, coupled-mode theory leads to the same analysis of EPDs as the CTL formulation presented in Section II and, therefore, can also be analyzed using bifurcation theory.

REFERENCES

[1] W. D. Heiss, "The physics of exceptional points," *J. Phys. A, Math. Theor.*, vol. 45, no. 44, p. 444016, 2012.

[2] C. M. Bender and S. Boettcher, "Real spectra in non-Hermitian Hamiltonians having $\mathscr{PT}$ symmetry," *Phys. Rev. Lett.*, vol. 80, no. 24, p. 5243, 1998.

[3] C. M. Bender, S. Boettcher, and P. N. Meisinger, "$\mathscr{PT}$-symmetric quantum mechanics," *J. Math. Phys.*, vol. 40, p. 2201, May 1999.

[4] C. E. Rüter, K. G. Makris, R. El-Ganainy, D. N. Christodoulides, M. Segev, and D. Kip, "Observation of parity–time symmetry in optics," *Nature Phys.*, vol. 6, pp. 192–195, Mar. 2010.

[5] H. Hodaei *et al.*, "Parity-time-symmetric coupled microring lasers operating around an exceptional point," *Opt. Lett.*, vol. 40, no. 21, pp. 4955–4958, Nov. 2015.

[6] M. A. K. Othman, V. Galdi, and F. Capolino, "Exceptional points of degeneracy and $\mathscr{PT}$ symmetry in photonic coupled chains of scatterers," *Phys. Rev. B, Condens. Matter*, vol. 95, no. 10, p. 104305, 2017.

[7] J. Doppler *et al.*, "Dynamically encircling an exceptional point for asymmetric mode switching," *Nature*, vol. 537, pp. 76–79, Sep. 2016.

[8] A. U. Hassan, B. Zhen, M. Soljačić, M. Khajavikhan, and D. N. Christodoulides, "Dynamically encircling exceptional points: Exact evolution and polarization state conversion," *Phys. Rev. Lett.*, vol. 118, p. 093002, Mar. 2017.

[9] C. A. Valagiannopoulos, "Optical PT-symmetric counterparts of ordinary metals," *IEEE J. Sel. Topics Quantum Electron.*, vol. 22, no. 5, p. 5000409, Sep./Oct. 2016.

[10] H. Hodaei *et al.*, "Enhanced sensitivity at higher-order exceptional points," *Nature*, vol. 548, pp. 187–191, Aug. 2017.

[11] D. L. Sounas, R. Fleury, and A. Alù, "Unidirectional cloaking based on metasurfaces with balanced loss and gain," *Phys. Rev. Appl.*, vol. 4, no. 1, p. 014005, 2015.

[12] F. Monticone, C. A. Valagiannopoulos, and A. Alù, "Parity-time symmetric nonlocal metasurfaces: All-angle negative refraction and volumetric imaging," *Phys. Rev. X*, vol. 6, no. 4, p. 041018, 2016.

[13] C. A. Valagiannopoulos, F. Monticone, and A. Alù, "PT-symmetric planar devices for field transformation imaging," *J. Opt.*, vol. 18, no. 4, p. 044028, 2016.

[14] M. Sakhdari, M. Farhat, and P.-Y. Chen, "PT-symmetric metasurfaces: Wave manipulation and sensing using singular points," *New J. Phys.*, vol. 19, p. 065002, Jun. 2017.

[15] T. Katō, *Perturbation Theory for Linear Operators*. Berlin, Germany: Springer-Verlag, 1995.

[16] A. Figotin and I. Vitebskiy, "Frozen light in photonic crystals with degenerate band edge," *Phys. Rev. E, Stat. Phys. Plasmas Fluids Relat. Interdiscip. Top.*, vol. 74, no. 6, p. 066613, 2006.

[17] A. Figotin and I. Vitebskiy, "Slow-wave resonance in periodic stacks of anisotropic layers," *Phys. Rev. A, Gen. Phys.*, vol. 76, no. 5, p. 053839, 2007.

[18] M. A. K. Othman, F. Yazdi, A. Figotin, and F. Capolino, "Giant gain enhancement in photonic crystals with a degenerate band edge," *Phys. Rev. B, Condens. Matter*, vol. 93, no. 2, p. 024301, 2016.

[19] J. L. Volakis and K. Sertel, "Narrowband and wideband metamaterial antennas based on degenerate band edge and magnetic photonic crystals," *Proc. IEEE*, vol. 99, no. 10, pp. 1732–1745, Oct. 2011.

[20] E. Hernández, A. Jaáuregui, A. Mondragón, and L. Nellen, "Degeneracy of resonances: Branch point and branch cuts in parameter space," *Int. J. Theor. Phys.*, vol. 46, no. 6, pp. 1666–1701, 2007.

[21] E. Hernández, A. Jáuregui, and A. Mondragón, "Exceptional points and non-Hermitian degeneracy of resonances in a two-channel model," *Phys. Rev. E, Stat. Phys. Plasmas Fluids Relat. Interdiscip. Top.*, vol. 84, no. 4, p. 046209, 2011.

[22] M. A. K. Othman and F. Capolino, "Theory of exceptional points of degeneracy in uniform coupled waveguides and balance of gain and loss," *IEEE Trans. Antennas Propag.*, vol. 21, no. 10, pp. 5289–5302, Oct. 2017.

[23] A. B. Yakovlev and G. W. Hanson, "On the nature of critical points in leakage regimes of a conductor-backed coplanar strip line," *IEEE Trans. Microw. Theory Techn.*, vol. 45, no. 1, pp. 87–94, Jan. 1997.

[24] G. W. Hanson and A. B. Yakovlev, "An analysis of leaky-wave dispersion phenomena in the vicinity of cutoff using complex frequency plane singularities," *Radio Sci.*, vol. 33, no. 4, pp. 803–819, 1998.

[25] A. B. Yakovlev and G. W. Hanson, "Analysis of mode coupling on guided-wave structures using Morse critical points," *IEEE Trans. Microw. Theory Techn.*, vol. 46, no. 7, pp. 966–974, Jul. 1998.

[26] A. B. Yakovlev and G. W. Hanson, "Fundamental modal phenomena on isotropic and anisotropic planar slab dielectric waveguides," *IEEE Trans. Antennas Propag.*, vol. 51, no. 4, pp. 888–897, Apr. 2003.

[27] G. W. Hanson and A. B. Yakovlev, "Investigation of mode interaction on planar dielectric waveguides with loss and gain," *Radio Sci.*, vol. 34, no. 6, pp. 1349–1359, 1999.

[28] A. B. Yakovlev and G. W. Hanson, "Mode-transformation and mode-continuation regimes on waveguiding structures," *IEEE Trans. Microw. Theory Techn.*, vol. 48, no. 1, pp. 67–75, Jan. 2000.

[29] G. Lovat, P. Burghignoli, A. B. Yakovlev, and G. W. Hanson, "Modal interactions in resonant metamaterial slabs with losses," *Metamaterials*, vol. 2, no. 4, pp. 198–205, 2008.

[30] A. B. Yakovlev and G. W. Hanson, "Modal propagation and interaction in the smooth transition from a metal mushroom structure to a bed-of-nails-type wire medium," *J. Appl. Phys.*, vol. 111, no. 7, p. 074308, 2012.

[31] G. W. Hanson, A. B. Yakovlev, and J. Hao, "Leaky-wave analysis of transient fields due to sources in planarly layered media," *IEEE Trans. Antennas Propag.*, vol. 51, no. 2, pp. 146–159, Feb. 2003.

[32] C. R. Paul, *Analysis of Multiconductor Transmission Lines*. Hoboken, NJ, USA: Wiley, 2008.

[33] G. Miano and A. Maffucci, *Transmission Lines and Lumped Circuits: Fundamentals and Applications*. San Francisco, CA, USA: Academic, 2001.

[34] R. F. Harrington, *Time-Harmonic Electromagnetic Fields*, vol. 8. New York, NY, USA: McGraw-Hill, 1961.

[35] M. A. K. Othman, V. A. Tamma, and F. Capolino, "Theory and new amplification regime in periodic multimodal slow wave structures with degeneracy interacting with an electron beam," *IEEE Trans. Plasma Sci.*, vol. 44, no. 4, pp. 594–611, Apr. 2016.

[36] D. G. Baranov, A. Krasnok, and A. Alù, "Coherent virtual absorption based on complex zero excitation for ideal light capturing," *Optica*, vol. 4, no. 12, pp. 1457–1461, 2017.

[37] C. E. Baum, "Emerging technology for transient and broad-band analysis and synthesis of antennas and scatterers," *Proc. IEEE*, vol. 64, no. 11, pp. 1598–1616, Nov. 1976.

[38] C. E. Baum, "The Singularity Expansion Method," in *Transient Electromagnetic Fields*, vol. 128, L. B. Felsen, Ed. New York, NY, USA: Springer-Verlag, 1976.

[39] P. Lancaster and M. Tismenetsky, *The Theory of Matrices*, 2nd ed. New York, NY, USA: Academic, 1985.
[40] C. D. Meyer, *Matrix Analysis and Applied Linear Algebra*. Philadelphia, PA, USA: SIAM, 2000, ch. 8.
[41] G. W. Hanson, A. I. Nosich, and E. M. Kartchevski, "Green's function expansions in dyadic root functions for shielded layered waveguide problems obtained via residue theory," *Prog. Electromagn. Res.*, vol. 39, pp. 61–91, 2003.
[42] M. Y. Nada, M. A. K. Othman, O. Boyraz, and F. Capolino, "Giant resonance and anomalous quality factor scaling in degenerate band edge coupled resonator optical waveguides," *J. Lightw. Technol.*, vol. 36, no. 14, pp. 3030–3039, Jul. 15, 2018.
[43] A. Welters, "On explicit recursive formulas in the spectral perturbation analysis of a Jordan block," *SIAM J. Matrix Anal. Appl.*, vol. 32, no. 1, pp. 1–22, 2011.
[44] R. Seydel, *Practical Bifurcation and Stability Analysis*, 2nd ed. New York, NY, USA: Springer-Verlag, 1994.
[45] M. Golubitsky and D. G. Schaeffer, *Singularities and Groups in Bifurcation Theory*, vol. 1. Berlin, Germany: Springer-Verlag, 1985.
[46] T. Poston and I. Stewart, *Catastrophe Theory and Its Applications*. London, U.K.: Sir Isaac Pitman, 1978.
[47] A. B. Yakovlev and G. W. Hanson, "Fundamental wave phenomena on biased-ferrite planar slab waveguides in connection with singularity theory," *IEEE Trans. Microw. Theory Techn.*, vol. 51, no. 2, pp. 583–587, Feb. 2003.
[48] H. Haus, W. Huang, S. Kawakami, and N. Whitaker, "Coupled-mode theory of optical waveguides," *J. Lightw. Technol.*, vol. 5, no. 1, pp. 16–23, 1987.
[49] M. A. K. Othman and F. Capolino, "Coupled transmission line array antennas with exceptional points of degeneracy," in *Proc. IEEE Int. Symp. Antennas Propag.*, San Diego, CA, USA, Jul. 2017, pp. 57–58.
[50] M. Y. Nada, M. A. K. Othman, and F. Capolino, "Theory of coupled resonator optical waveguides exhibiting high-order exceptional points of degeneracy," *Phys. Rev. B, Condens. Matter*, vol. 96, no. 18, p. 184304, 2017.
[51] M. A. K. Othman, X. Pan, G. Atmatzakis, C. G. Christodoulou, and F. Capolino, "Experimental demonstration of degenerate band edge in metallic periodically loaded circular waveguide," *IEEE Trans. Microw. Theory Techn.*, vol. 65, no. 11, pp. 4037–4045, Nov. 2017.
[52] A. Guo *et al.*, "Observation of PT-symmetry breaking in complex optical potentials," *Phys. Rev. Lett.*, vol. 103, no. 9, p. 093902, 2009.

Authors' photographs and biographies not available at the time of publication.